VNU Journal of Science: Mathematics - Physics

Journal homepage: https://js.vnu.edu.vn/MaP

Original Article

Fabrication oF SnS_2/Graphene Electrode Using Hydrothermal Method Towards Supercapacitor Applications

Han Thi Thu[1], Nguyen Thi Phuong Nhung[2], Chu Manh Hung[1], Dao Xuan Viet[1], Chu Thi Xuan[1,*], Nguyen Duc Hoa[1]

[1]*School of Materials Science and Engineering (SMSE), Hanoi University of Science and Technology, 1 Dai Co Viet, Hai Ba Trung, Hanoi, Vietnam*

[2]*Petro Vietnam University, 672 Cach Mang Thang Tam, Long Toan, Ba Ria, Ba Ria Vung Tau, Vietnam*

Received 31st July 2025
Revised 6th September 2025; Accepted 17th January 2026

Abstract: In the context of climate change and the growing demand for energy, supercapacitors are regarded as one of the key technologies for enabling a sustainable future. In this study, Tin disulfide (SnS_2) nanomaterials were synthesized via a hydrothermal method and employed as electrode materials in supercapacitor. The morphology and composition of the synthesized materials were investigated using scanning electron microscopy, energy dispersive X-ray spectroscopy, and X-ray diffraction spectroscopy. The electrochemical performance of both SnS_2 and SnS_2/Graphene composite electrodes was measured in 2M KOH electrolyte using cyclic voltammetry (CV), galvanostatic charge-discharge (GCD), and electrochemical impedance spectroscopy (EIS). The SnS_2/Graphene electrode exhibited a high specific capacitance of 265.97 F/g at a scan rate of 5 mV/s and 280.5 F/g at a current density of 1 A/g, along with energy and power densities of 19.05 Wh/kg and 354 W/kg, respectively. These findings show that the fabricated electrode is a promising candidate for sustainable energy storage systems.

Keywords: Supercapacitor; SnS_2/Graphene composite electrodes; SnS_2 electrodes; Electrochemistry.

1. Introduction

The increasing global demand for energy, driven by economic growth and technological advancements, has accelerated the depletion of fossil fuel resources. As a result, renewable energy sources have gained significant attention and are being increasingly harnessed. However, due to their dependence on natural conditions, renewable energy sources often exhibit lower stability and reliability

* Corresponding author.
E-mail address: xuan.chuthi@hust.edu.vn

https//doi.org/10.25073/2588-1124/vnumap.5055

compared to conventional energy systems. This challenge underscores the urgent need for efficient energy storage devices to balance supply and demand [1]. Supercapacitors have emerged as advanced energy storage devices that combine the advantages of traditional capacitors and batteries, offering a promising alternative to conventional battery technology. With their fast charging, discharging capabilities, long cycle life, and high-power density, supercapacitors are being increasingly applied in various fields, including portable electronics, electric vehicles, and renewable energy systems. Nanocomposite materials such as graphene and metal oxides are widely used in the development of high-performance supercapacitor electrodes [2].

Among various materials, Tin (IV) sulfide (SnS_2) has emerged as a promising candidate for supercapacitor applications due to its unique layered structure, large specific surface area, and environmental friendliness [3]. Recent research has increasingly focused on the development of supercapacitors using SnS_2-based materials [4]. In 2021, Mahboobeh Setayeshmehr et al., [4] reported the synthesis of three-dimensional (3D) flower-like SnS_2 structure using a hydrothermal method, with alkali-doped SnS_2 to enhance electrochemical performance. Their findings demonstrated that sodium-doped SnS_2 exhibited the highest capacitance of 269 F/g at a current density of 1 A/g in a three-electrode system [4].

However, the practical application of SnS_2 in supercapacitors is hindered by its inherently low electrical conductivity and limited structural stability, which restrict the electron transfer rate and overall electrochemical performance. To address these limitations, graphene has been introduced as a complementary material due to its exceptional electrical conductivity and its ability to serve as a robust structural framework [5]. The incorporation of Graphene significantly enhances structural integrity and facilitates faster electron transport, thereby accelerating the charging and discharging processes. Furthermore, the large specific surface area of graphene contributes to improved ion storage capacity and overall energy storage performance [6].

In 2010, Liu et al., [7] investigated the use of graphene-based electrodes in supercapacitors. Their study demonstrated promising cycling stability, with less than a 10% decrease in capacitance after 500 charge-discharge cycles. They also highlighted the potential for further enhancement of cycle life through optimization of electrode materials. Even at a high current density of 4 A/g, the graphene electrode maintained a relatively high energy density of 60 Wh/kg [7]. Although extensive research has been conducted on the fabrication of supercapacitors using either SnS_2 or graphene individually, few studies have explored the combination of these two materials. The integration of SnS_2 with graphene holds significant promise, as the synergistic combination of SnS_2's layered structure and graphene's superior conductivity may result in improved electrochemical performance for supercapacitor applications.

In this study, we present a simple and efficient hydrothermal method for the synthesis of SnS_2 nanomaterials. These materials are subsequently employed to fabricate two types of electrodes, pure SnS_2 and SnS_2/Graphene composites, which are evaluated for their electrochemical properties using three-electrode system in an alkaline medium. The resulting device, based on the layered architecture of SnS_2/Graphene demonstrates strong potential as an advanced electrode material for future energy storage applications.

2. Experimental

2.1. Synthesis of SnS_2 Nanostructures

The SnS_2 nanomaterials were synthesized via one-step hydrothermal method using hydrochloric acid (HCl), Tin (IV) chloride pentahydrate ($SnCl_4 \cdot 5H_2O$), and thiourea (CH_4N_2S) as precursors. The

fabrication procedure is illustrated in Figure 1. All chemical agents were purchased from Sigma Aldrich with the purity of ≥ 99.9% and were used as received without further purification.

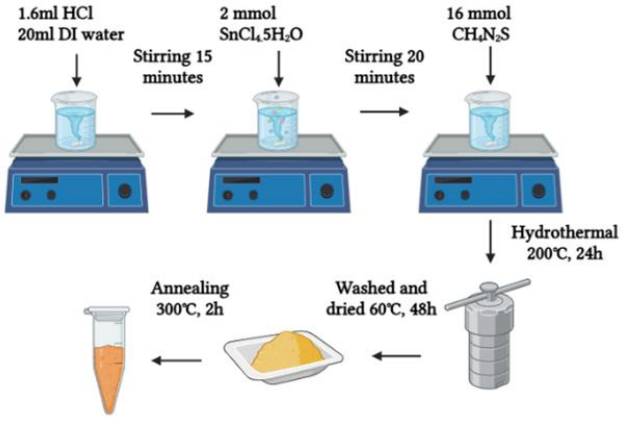

Figure 1. Fabrication process of SnS_2 nanomaterials by hydrothermal method.

Initially, 1 mmol $SnCl_4.5H_2O$ was dissolved in an HCl solution and stirred for 15 minutes to obtain a homogenous mixture. Subsequently, 8 mmol Thiourea was added to the solution, and continuous stirring was performed until the pH of the mixture reached approximately 1. During this process, the solution gradually transformed from a dense to transparent state. The resulting mixture was then transformed into a 100 mL Teflon-lined stainless-steel autoclave and subjected to hydrothermal treatment in an electric furnace at 200°C for different time, ranging from 16 to 26 hours. After the reaction, the autoclave was allowed to cool naturally to room temperature. The yellow precipitates obtained were collected and thoroughly washed several times with deionized water and ethanol to remove any residual impurities. The washed products were then dried in an electric oven at 60°C for 48 hours. Finally, the dried powders were annealed at 300°C for 2 hours under a continuous flow of argon gas (50 sccm) to enhance crystallinity and purity, yielding the final yellow SnS_2 product for subsequent characterization.

2.2. Synthesis of SnS_2 and SnS_2/Graphene Electrodes

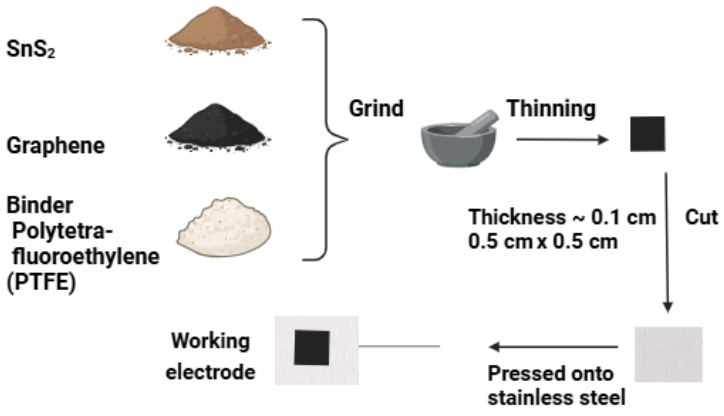

Figure 2. Electrode fabrication process.

A stainless-steel substrate with dimensions of 1 cm × 1 cm × 0.1 cm (width x length x thickness) was pre-treated in an HCl solution to remove surface impurities. The treated stainless steel was then thoroughly rinsed multiple times with ethanol and deionized (DI) water to ensure surface cleanliness.

The synthesized SnS_2 powder was employed as the electroactive material, while graphene served as a conductive additive to enhance electrical performance. A composite mixture containing SnS_2, graphene, and Polytetrafluoroethylene (PTFE) binder in a weight ratio of 80:10:10 was prepared and homogenized using ball milling for 2 hours. The resulting slurry was pressed into disks under a pressure of 9800 kPa, and subsequently rolled into thin electrode sheet, as illustrated in Figure 2. For comparison, a pure SnS_2 electrode was fabricated using a mixture of SnS_2 and PTFE in a weight ratio of 90 :10, following the same procedure.

Square electrodes with dimensions of 0.5 cm × 0.5 cm and a thickness of 0.1 cm were cut from the prepared electrode sheets and pressed onto stainless steel mesh under a pressure of 9800 kPa to form the working electrodes. The mass loading of the active material on each working electrode was approximately 0.002 g.

2.3. Electrochemical Measurements

The electrochemical performance of the fabricated electrodes was evaluated using a three-electrode configuration on an Autolab electrochemical workstation. A Platinum wire and a Hg/HgO electrode were utilized as the counter electrode and reference electrode, respectively. The electrochemical behavior of the prepared electrodes was investigated through cyclic voltammetry (CV), galvanostatic charge–discharge (GCD), and electrochemical impedance spectroscopy (EIS). GCD and CV measurements were conducted within potential windows ranging from −0.2 to –0.5 V, at various current densities (1–10 A/g) and scan rates (5–100 mV/s). EIS measurements were performed under the following conditions: an AC voltage amplitude of 10 mV and a frequency range from 0.01 Hz to 200 kHz. Based on the obtained data, the specific capacitance, C_s (F/g), energy density, E (Wh/kg) and power density, P (W/kg) of the electrodes were calculated using following equations [8]:

$$C_2 = \frac{1}{sm\Delta V}\int_{V_1}^{V_2} I(V)dV = \frac{A}{sm\Delta V} \quad (1)$$

$$C_s = \frac{I\Delta t}{m\Delta V} \quad (2)$$

where Δt (s) represents the discharge time, I (A) represents the applied current during the charge/discharge process, m (g) is the mass of the active electrode material, C_s (F/g) refers to the specific capacitance, and ΔV (V) corresponds to the potential window of the electrode material.

3. Results and Discussion

3.1. Morphology and Structure of SnS_2 Nanoflakes

The morphology of the SnS_2 materials synthesized at a constant temperature of 200°C but with varying reaction times from 16 to 26 hours was investigated using scanning electron microscopy (SEM). As shown in Figure 3, all samples exhibited a characteristic hexagonal sheet-like structure with relatively uniform particle sizes and well-defined particle boundaries.

The particle size distribution of the synthesized SnS_2 samples was analyzed using ImageJ software. As shown in Figure 4, the particle diagonal sizes ranged from 6 to 14 μm. Notably, the SnS_2 nanosheets synthesized under hydrothermal conditions at 200°C for 24 hours exhibited a more uniform and well-defined size distribution (Figure 4). This uniformity is attributed to the optimized hydrothermal reaction

time, which promotes controlled recrystallization and facilitates the formation of SnS_2 crystals with more stable, consistent sizes and morphologies.

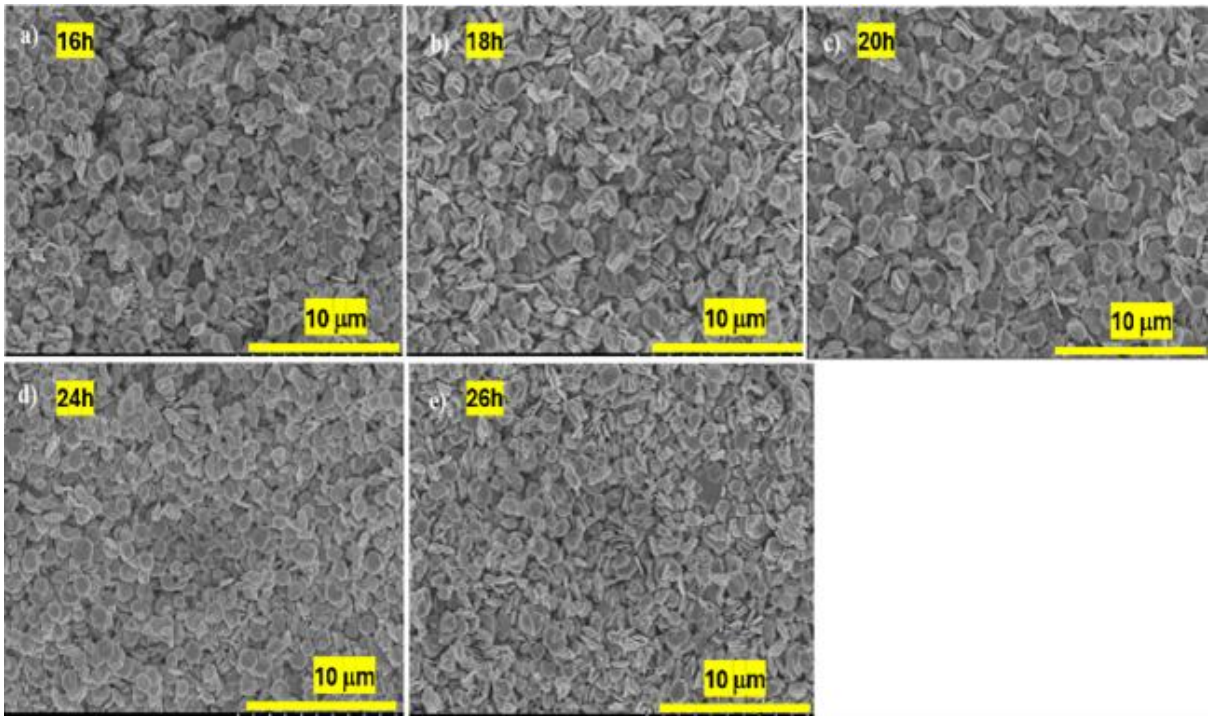

Figure 3. SEM images of hydrothermally synthesized SnS_2 samples at 200°C with corresponding times of (a) 16h, (b) 18h, (c) 20h, (d) 24h, and (e) 26h.

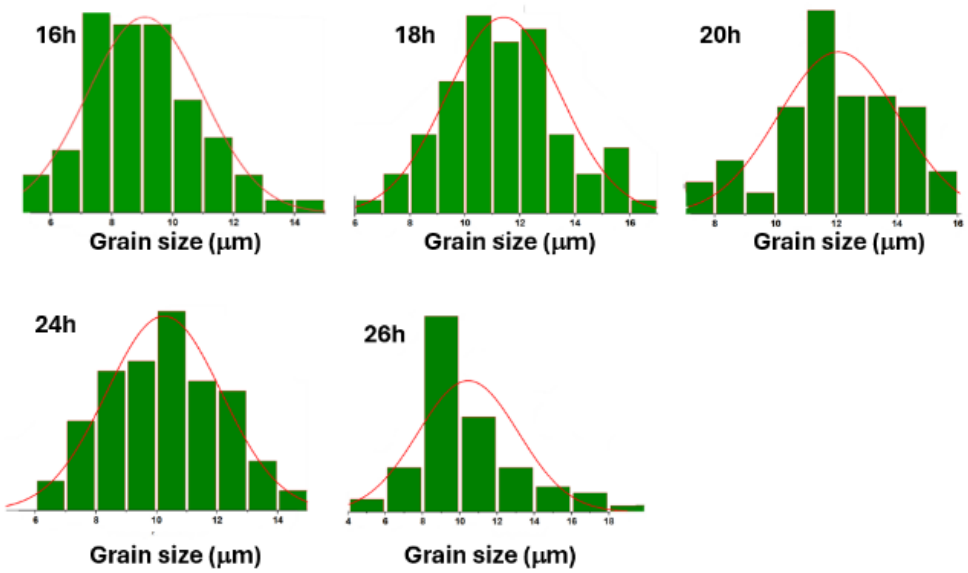

Figure 4. Analysis of SnS_2 material crystal size hydrothermally synthesized at 200°C from 16 to 26 hours using ImageJ.

To examine the sample composition, the X-ray diffraction (XRD) and energy-dispersive X-ray spectroscopy (EDS) measurements were performed. As shown in Figure 5, all diffraction peaks observed at 2θ values of 14.46°, 27.75°, 31.64°, 41.5°, and 49.55°, correspond to the (001), (100), (101), (102), and (110) crystal planes, respectively [9]. These diffraction peaks can be clearly indexed to the hexagonal phase of SnS_2 and are consistent with standard reference data for SnS_2 (JCPDS card no. 23-0677). No additional peaks associated with impurities were detected in the XRD patterns, confirming the high phase purity of the synthesized materials.

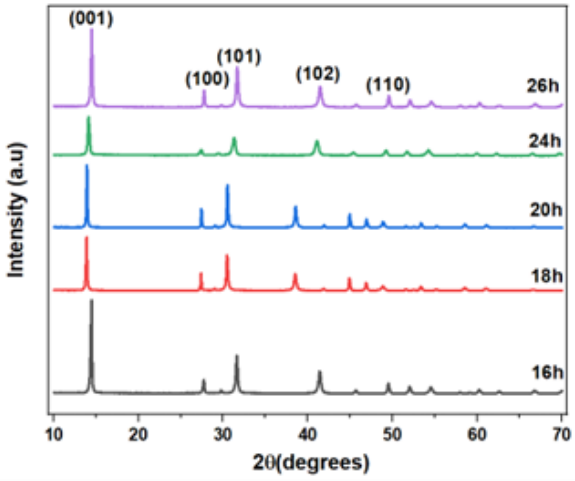

Figure 5. X-ray diffraction patterns of SnS_2 samples with different hydrothermal times.

The composition of the synthesized nanostructures was further investigated using EDS technique, as shown in Figure 6. The EDS results confirm the presence of Tin (Sn) and sulfur (S) with atomic percentages of 66.66% and 33.34%, respectively. The atomic ratio of Sn:S is approximately 1:2, indicating that the synthesized product predominantly consists of SnS_2, which is in good agreement with previous reports [10]. The results further confirm the successful synthesis of high-purity and homogenous SnS_2 nanoflakes.

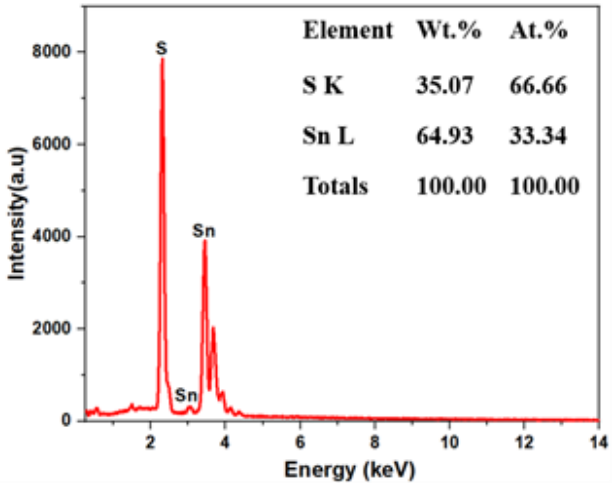

Figure 6. EDS analysis of the synthesized electrode.

3.2. Electrochemical Behaviors

3.2.1. CV measurement of SnS_2 and SnS_2/Graphene Electrodes

The cyclic voltammetry (CV) measurements of the SnS_2 electrodes were performed in 2M KOH electrolyte over a potential window from -0.2 to 0.5 V at scan rates ranging from 5 to 100 mV/s, as shown in Figure 7. In all cases, well-defined redox peaks are clearly observed, indicating the occurrence of sequentially redox reactions. The oxidation peaks appear at approximately 0.26 V during the discharge process, while the corresponding reduction peaks are observed around 0.01 V during the charge process. In general, with increasing scan rates, the redox peak pairs broaden, and the enclosed area of the CV curves increase, reflecting typical pseudocapacitive behavior [11]. This behavior demonstrates that the electrochemical charge storage mechanism of the SnS_2 electrode involves both faradaic redox reactions and capacitive characteristics.

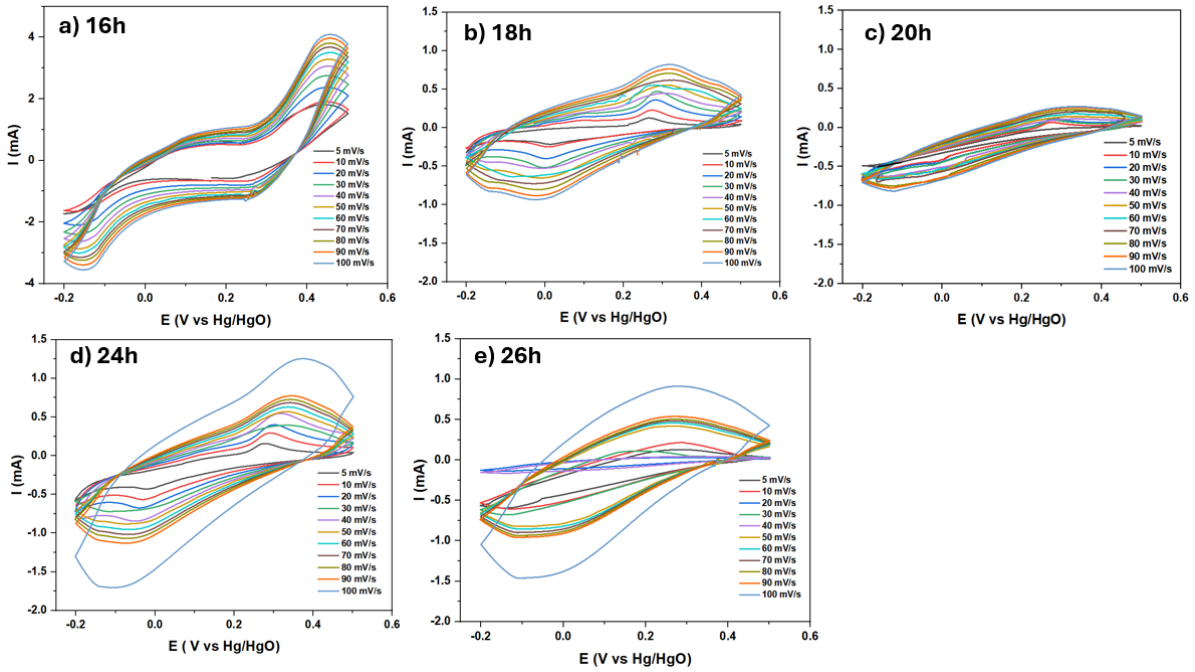

Figure 7. CV curves at different scan rates using SnS_2 as the electrode with hydrothermal times of a) 16h; b) 18h; c) 20h; d) 24h; e) 26h, respectively.

At a hydrothermal reaction time of 16 hours (Figure 7a), redox peaks are present but poorly defined. The short reaction time likely results in incomplete phase formation. In Figure 7b, corresponding to the sample synthesized for 18 hours, distinct oxidation and reduction peaks appear at approximately 0.26 V and 0.01 V, respectively, though the current intensity remains relatively low. When the reaction time reaches 20h (Figure 7c), the CV curve exhibits noticeable noise and less distinct redox peaks, suggesting the presence of some impurities and indicating that the phase formed under these conditions is unstable. In contrast, as shown in Figure 7d, the materials synthesized for 24h display clear redox peak pairs like those in Figure 7b but significantly higher current densities, demonstrating improved electrochemical performance. Finally, the sample prepared with hydrothermally time of 26 hours (Figure 7e) shows a decline in current density compared to 24 hours,

indicating that prolonged reaction times may lead to structural or compositional changes that negatively affect charge storage performance.

These results indicate that, under hydrothermal condition at 200°C, a reaction time of 24 hours yields the most stable CV responses, confirming that the hydrothermal time significantly influences the electrochemical characteristics of the SnS_2 electrodes.

The CV curve of the SnS_2/Graphene electrode, shown in Figure 8, exhibits broader and more pronounced redox peaks due to the presence of graphene within the electrode composition. Like the SnS_2 electrode (Figure 7), the SnS_2/Graphene electrode shows oxidation peaks at approximately 0.28 V, and reduction peaks at around - 0.02 V, with symmetrical redox peak pairs relative to the potential axis. Notably, the SnS_2/graphene electrode demonstrates a high current density compared to the pure SnS_2 electrode. This enhancement in current density results is attributed to the excellent electrical conductivity and improved electron transfer pathways provided by the graphene network.

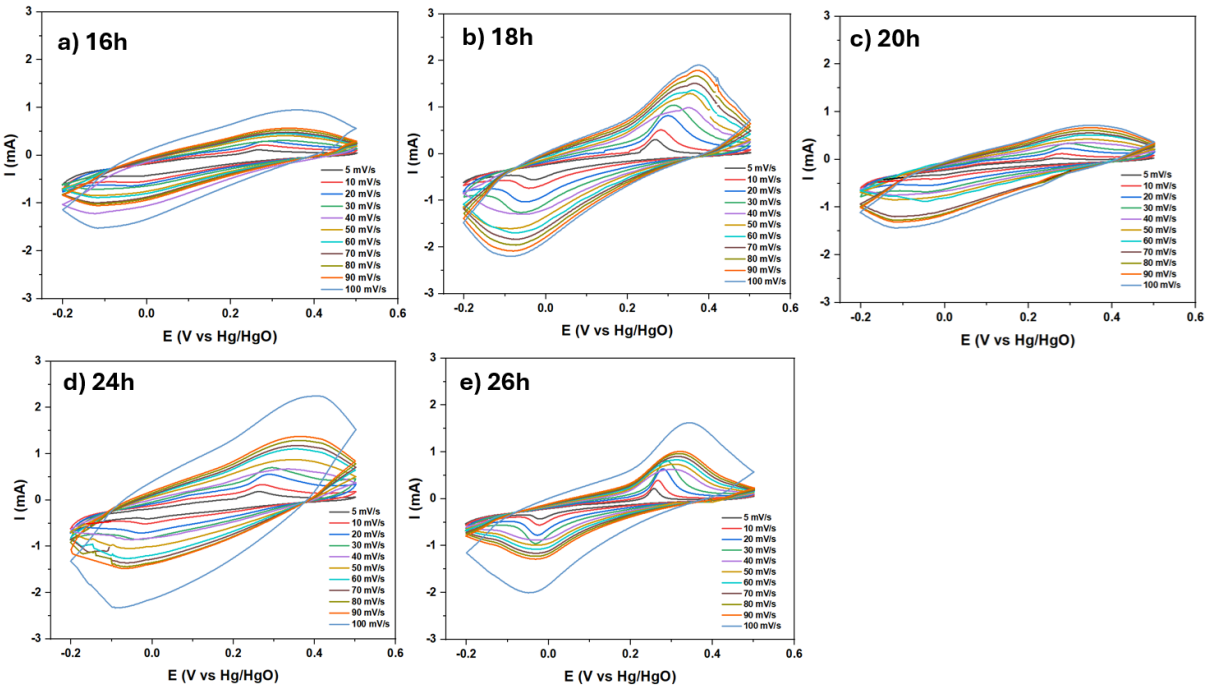

Figure 8. CV curves at different scan rates using SnS_2/Graphene as the electrode with hydrothermal times of a) 16h; b) 18h; c) 20h; d) 24h; e) 26h, respectively.

The symmetry of redox peak pairs indicates facile ion adsorption and desorption at the electrode surface, with minimal or negligible side reactions. The consistent appearance of these redox peaks across multiple scan cycles further demonstrates the high electrochemical stability of the electrode material. Among the SnS_2/Graphene electrodes, the sample synthesized with 24 hours hydrothermal treatment exhibits the highest and most stable current intensity and was therefore selected for further investigation.

To further evaluate the electrochemical performance of the SnS_2 and SnS_2/Graphene composite materials, the specific gravimetric capacitances of their electrodes were calculated from the CV curves using the Equation (1). The corresponding results are presented in Figure 9. As expected, the specific capacitances of both SnS_2 and SnS_2/Graphene electrodes gradually decreased with increasing scan rate, which is typical behavior for pseudocapacitive materials. Notably, the specific capacitances of the SnS_2/Graphene electrode (Figure 9b) were consistently higher than those of the pure SnS_2 electrode

without Graphene (Figure 9a), highlighting the beneficial role of graphene in enhancing charge storage capability.

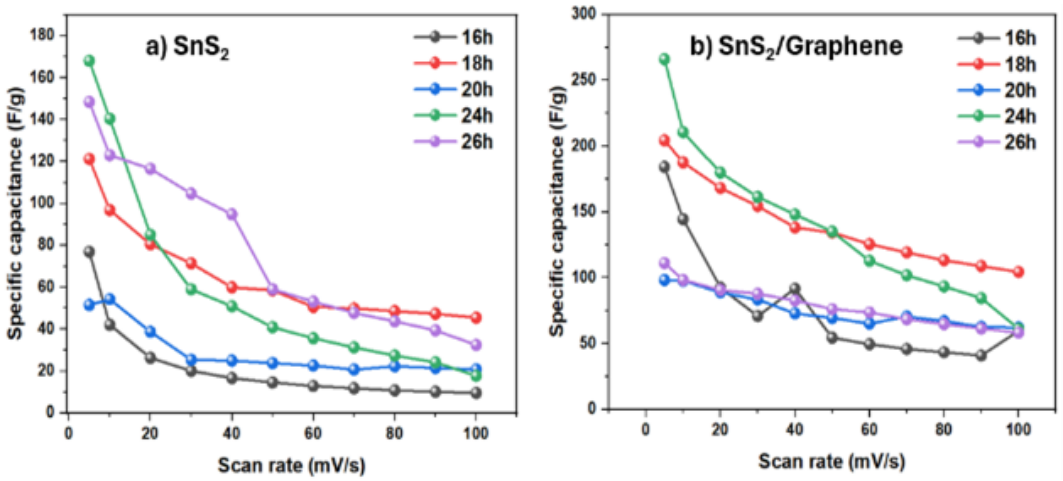

Figure 9. Specific capacitance of electrode samples synthesized under different hydrothermal conditions at scan rates ranging from 5 – 100 mV/s: a) SnS_2 electrode; b) SnS_2/Graphene electrode.

Thus, the incorporation of graphene significantly improves the specific capacitance of the SnS_2/Graphene electrode. These results indicate that the presence of carbon materials, such as graphene, has a positive impact on the capacitance behavior of supercapacitor by improving conductivity and facilitating charge transfer. At the lowest scan rate, both SnS_2 and SnS_2/Graphene electrodes synthesized via a 24 h hydrothermally process exhibit the highest specific capacitance values.

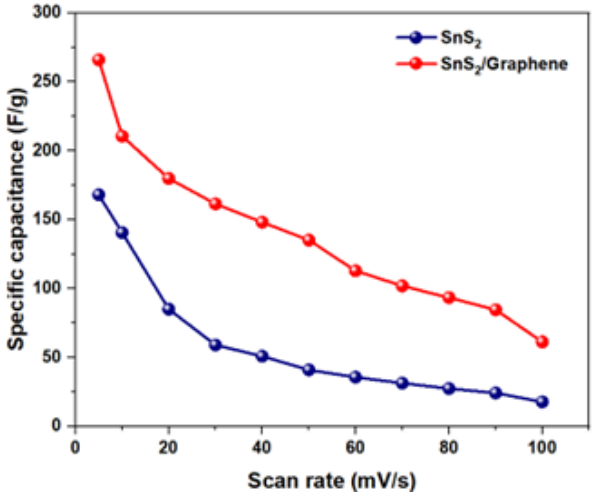

Figure 10. Specific capacitance of the SnS_2 and SnS_2/Graphene electrodes synthesized under hydrothermal condition of 24 hours, measured at scan rates ranging from 5 – 100 mV/s.

To further highlight the performance differences between the SnS_2 and SnS_2/Graphene electrodes prepared under identical hydrothermal conditions, a comparative analysis is presented in Figure 10.

As shown in Figure 10, SnS_2 sample shows the highest specific capacitance of 167.99 F/g at a scan rate of 5 mV/s, which gradually decreases with increasing scan rates due to limited ion diffusion within the electrode materials. In contrast, the SnS_2/Graphene electrode achieves a higher specific capacitance of 265.97 F/g at 5 mV/s and maintains a relatively high value of 61.19 F/g even at 100 mV/s. At higher scan rates, the diffusion process of ions in the electrolyte solution becomes insufficient to sustain the redox reactions, leading to a decrease in specific capacitance and reduced device efficiency [12].

To further confirm the critical role of carbon in the SnS_2/Graphene electrode, electrochemical impedance spectroscopy (EIS) measurements were performed on both SnS_2 and SnS_2/Graphene electrodes prior to cycling, at open-circuit potential (OCP). As shown in Figure 11, the Nyquist of both electrodes display a single semicircle in mid-frequency region, which corresponds to the charge-transfer resistance (Rct) at the electrode-electrolyte interface. The diameter of the semicircle for the SnS_2/Graphene electrode is noticeably smaller than that of the pure SnS_2 electrode, indicating a lower charge-transfer resistance. Impedance fitting results reveal that the SnS_2/Graphene electrode exhibits an Rct of 1.86 Ω, which is lower than the 2.02 Ω observed for the SnS_2 electrode. This reduction in charge transfer resistance suggests that the presence of graphene enhances electron transport across the electrode-electrolyte interface, thereby improving the electrode's overall electrochemical performance. The enhanced electron transfer in the SnS_2/graphene electrode contributes to its higher specific capacitance, as previously shown in Figure 10.

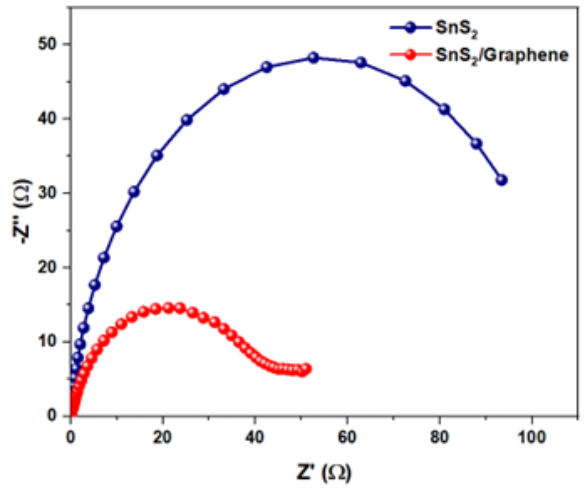

Figure 11. Nyquist plots of SnS_2 and SnS_2/Graphene electrodes in KOH electrolyte and equivalent circuit.

These results suggest that the presence of carbon in SnS_2/Graphene composite provides fast charge transfer pathways at the SnS_2 electrode-electrolyte interface, confirming the crucial role of carbon in enhancing the electrochemical performance of the SnS_2/graphene electrode.

3.2.2. Discharge-charge Characteristics of SnS_2 and SnS_2/Graphene Electrodes Synthesized with a 24h Hydrothermal Treatment

The galvanostatic charge-discharge (GCD) curves of the SnS_2 electrode at various current densities, presented in Figure 12a, reveal significantly shorter charge-discharge time (127 seconds) compared to the SnS_2/Graphene electrode, which exhibits longer discharge times of approximately 319 seconds. As shown in Figure 12b, the GCD curves of both electrodes at a current density of 1 A/g display distinct voltage plateaus at approximately 0.28 V and -0.02 V.

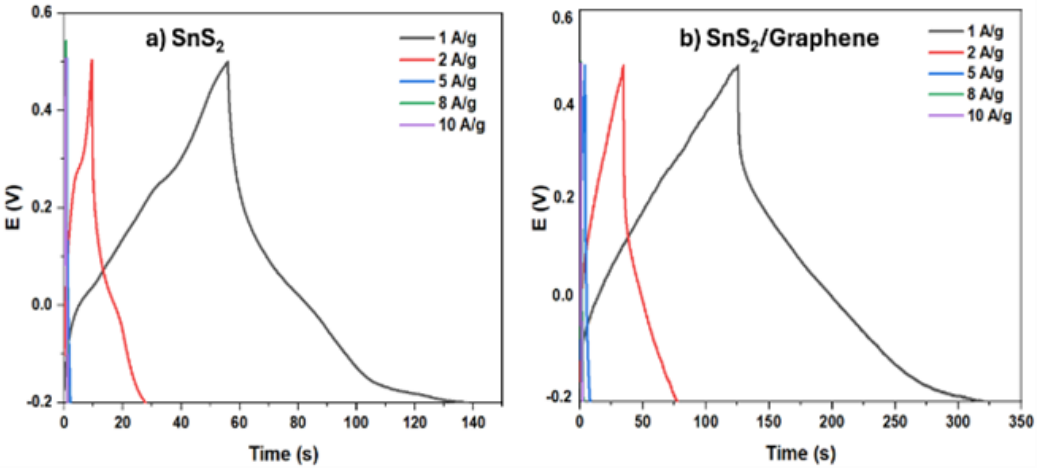

Figure 12. GCD curves of (a) SnS_2 electrode and (b) SnS_2/Graphene electrode.

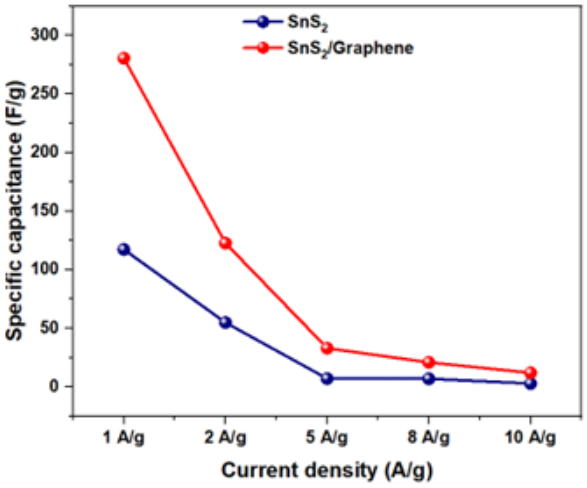

Figure 13. Specific capacitance of SnS_2 and SnS_2/Graphene electrodes at different current densities.

These observations are consistent with the redox peaks observed in the CV curves (Figure 7 and Figure 8), confirming that the capacitance arises from a combination of electric double-layer capacitor (EDLC) and pseudo-capacitance contributions. Furthermore, the GCD curves at varying current densities maintain relatively good symmetry between the charge and discharge segments, indicating excellent electrochemical reversibility. Even at a high current density of 10 A/g, the curves retain this symmetry, demonstrating the electrodes' good rate capability. The specific capacitance of the electrode materials was calculated using Equation (2).

The specific capacitance values, calculated from the charge-discharge curves (Figure 13), show a gradual decrease with increasing current density across all tested values (1, 2, 5, 8, and 10 A/g). At a current density of 1 A/g, the SnS_2/Graphene electrode exhibits a significantly higher specific capacitance of 280.5 F/g compared to 117.3 F/g for the SnS_2 electrode. This sustainable improvement is attributed to the optimal hydrothermal synthesis conditions, the enhanced electrode architecture, and the increased surface area provided by graphene, which collectively contributed to reduce internal resistance and improve charge storage performance. Owing to these superior properties, supercapacitors using

SnS_2/graphene composite electrodes show strong potential for practical applications in diverse fields such as electric vehicles, mobile electronic devices, and energy storage systems.

Table 1. Comparison of results obtained in this study with previous research on supercapacitor using SnS_2-based electrode materials [14]

Materials / Synthesis method	Electrolyte solution	Specific capacitance (F/g)	Ref.
SnS_2 Solvothermal	1 M KCl	215.9 @ 0.38 A/g	[15]
SnS_2 Hydrothermal	3M KOH	177 @ 1 A/g	[16]
SnS_2 Solvothermal	0.5M Na_2SO_4	65 @ 2 A/g	[17]
SnS_2 Solvothermal	6M KOH	108.6 @ 1 A/g	[18]
SnS_2 Hydrothermal	0.5M KOH	93 @ 1 A/g	[19]
Graphene Chemical method	EMIMBF4	270 @ 1 A/g	[7]
SnS_2 Hydrothermal	2M KOH	117.3 @ 1 A/g	This study
SnS_2/Graphene Hydrothermal	2M KOH	280.5 @ 1 A/g	This study

Comparison of the electrochemical performance of the SnS_2/graphene electrode developed in this study with recent studies on SnS_2-based supercapacitors is shown in Table 1. The SnS_2/Graphene electrode fabricated in this work exhibited a significantly higher specific capacitance than those reported in previous studies. This enhancement is primarily attributed to the incorporation of graphene, which improves electrical conductivity, facilitates faster electron and ion transport, and increases the overall charge storage capability of the electrode. These findings demonstrate that the SnS_2/Graphene composite electrode delivers excellent electrochemical performance in an alkaline electrolyte, highlighting its potential for practical application in next-generation energy storage devices.

4. Conclusion

SnS_2 and SnS_2/Graphene electrodes were successfully synthesized via a simple and efficient hydrothermal method with reaction time ranging from 16 to 26 hours. Structure characterization revealed that SnS_2 synthesized at 200°C for 24 hours exhibited the most favorable morphology. Electrochemical evaluations demonstrated the superior performance of the SnS_2/Graphene electrode compared to the pure SnS_2 electrode, which is attributed to its larger surface area and enhanced conductivity. Specifically, the SnS_2/Graphene electrode achieved a high specific capacitance of 265.97 F/g at a scan rate of 5 mV/s and 280.5 F/g at a current density of 1 A/g. These results suggest that the improved specific capacitance of the SnS_2/Graphene composite makes it a promising candidate for future supercapacitor applications.

Acknowledgments

This research is funded by the Ministry of Science and Technology of Vietnam under Grant No. ĐTĐL.CN-35/23.

References

[1] Z. Salameh, Chapter 4 – Energy Storage, Renewable Energy System Design, 2014.

[2] K. Oyedotun, Supercapacitor: History, Types, Materials, Processes, Evaluations and Applications, nECS Meeting Abstracts, Vol. MA2022-02, No. 6, 2022, https//doi.org/10.1149/ma2022-026605mtgabs.

[3] J. Li, L. Li, Y. Du, X. Liu, L. Wang, Carbon Spheres Decorated with SnS2 Nanosheets as a Low-cost Counter-electrode Material for Dye-sensitized Solar Cell, Mater Lett, Vol. 363, 2024, pp. 136239, https//doi.org/10.1016/J.Matlet.2024.136239.

[4] M. Setayeshmehr, M. Haghighi, K. Mirabbaszadeh, Binder-free 3D Flower-like Alkali Doped- SnS2 Electrodes for High-performance Supercapacitors, Electrochim Acta, Vol. 376, 2021, pp. 137987, https//doi.org/ 10.1016/J.Electacta.2021.137987.

[5] X. Fu, Y. Liu, X. Wang, L. Kang, T. Qiu, Graphene-based Advanced Materials for Energy Storage and Conversion Systems: Progress, Challenges, and Commercial Future, Appl Energy, Vol. 386, 2025, pp. 125566, https//doi.org/10.1016/J.Apenergy.2025.125566.

[6] S. Feng, X. Li, C. Shang, L. Tang, J. Zhang, Germanium Based Glass Modified by Graphene as Anode Material with High Capacity for Lithium-ion Batteries, J Non Cryst Solids, Vol. 646, 2024, pp. 123257, https//doi.org/10.1016/J.Jnoncrysol.2024.123257.

[7] C. Liu, Z. Yu, D. Neff, A. Zhamu, B. Z. Jang, Graphene-based Supercapacitor with an Ultrahigh Energy Density, Nano Lett, Vol. 10, No. 12, 2010, https//doi.org/10.1021/nl102661q.

[8] M. R. Pallavolu, Y. Anil Kumar, G. Mani, R. A. Alshgari, M. Ouladsmane, S. W. Joo, Facile Fabrication oOf Novel Heterostructured Tin Disulfide (SnS2)/tin Sulfide (SnS)/N-CNO Composite with Improved Energy Storage Capacity for High-performance Supercapacitors, Journal of Electroanalytical Chemistry, Vol. 899, 2021, pp. 115695, https//doi.org/10.1016/J.Jelechem.2021.115695.

[9] Z. Wang, Y. Chen, L. Yao, C. Zheng, M. Wang, One-step Hydrothermal Synthesis of Cu Doped SnS2 Quantum Dots Anchored on Reduced Graphene Oxide (rGO) as High-performance Electrodes for Supercapacitors, J Alloys Compd, Vol. 973, 2024, pp. 172906, https//doi.org/10.1016/J.Jallcom.2023.172906.

[10] Q. M. A. Bataineh et al., Cobalt-doped SnS2 Nanoplates for High-efficiency Catalysis Applications, Mater Chem Phys, Vol. 317, 2024, pp. 129184, https//doi.org/10.1016/J.Matchemphys.2024.129184.

[11] P. Saini, A Historical Review of Electrode Materials and Electrolytes for Electrochemical Double Layer Supercapacitors and Pseudocapacitors, Indian Journal of Pure and Applied Physics, Vol. 61, No. 4, 2023, https//doi.org/10.56042/ijpap.v61i4.69622.

[12] Z. Sun, M. Cao, W. Gao, Electrochemical Kinetic Evolution of Electrically Neutral Redox Mediator in Electrolyte Toward Advanced Electrochemical Energy Storage Device, J Power Sources, Vol. 640, 2025, pp. 236700, https//doi.org/10.1016/J.Jpowsour.2025.236700.

[13] I. Beyers, A. Bensmann, R. H. Rauschenbach, Ragone Plots Revisited: a Review of Methodology and Application Across Energy Storage Technologies, 2023, https//doi.org/10.1016/j.est.2023.109097.

[14] S. A. Thomas, J. Cherusseri, Strategically Designing Layered Two-dimensional SnS2-based Hybrid Electrodes: a Futuristic Option for Low-cost Supercapacitors, Journal of Energy Chemistry, Vol. 85, 2023, pp. 394-417, https//doi.org/10.1016/J.Jechem.2023.06.037.

[15] R. K. Mishra, G. W. Baek, K. Kim, H. I. Kwon, S. H. Jin, One-step Solvothermal Synthesis of Carnation Flower-Like SnS2 as Superior Electrodes for Supercapacitor Applications, Appl Surf Sci, Vol. 425, 2017, pp. 923-931, https//doi.org/10.1016/J.Apsusc.2017.07.045.

[16] Y. Xu, Y. Zhou, J. Guo, S. Zhang, Y. Lu, Preparation of SnS2/g-C3N4 Composite as the Electrode Material for Supercapacitor, J Alloys Compd, Vol. 806, 2019, pp. 343-349, https//doi.org/10.1016/J.Jallcom.2019.07.130.

[17] P. Asen, M. Haghighi, S. Shahrokhian, N. Taghavinia, One Step Synthesis of SnS2-SnO2 Nano-heterostructured as an Electrode Material for Supercapacitor Applications, J Alloys Compd, Vol. 782, 2019, pp. 38-50, https//doi.org/10.1016/J.Jallcom.2018.12.176.

[18] H. Chu, F. Zhang, L. Pei, Z. Cui, J. Shen, M. Ye, Ni, Co and Mn Doped SnS2-graphene Aerogels for Supercapacitors, J Alloys Compd, Vol. 767, 2018, pp. 583-591, https//doi.org/10.1016/J.Jallcom.2018.07.126.

[19] B. Wang et al., 2D/2D SnS2/MoS2 Layered Heterojunction for Enhanced Supercapacitor Performance, Journal of the American Ceramic Society, Vol. 103, No. 2, 2020, https//doi.org/10.1111/jace.16778.